The International Journal of Advanced Manufacturing Technology
https://doi.org/10.1007/s00170-026-18092-8

ORIGINAL ARTICLE

Effect of liquid CO_2 flow rate on TiAlN coated tools in hard turning of 42CrMo4 steel

Matej Drobnič[1,2] · Luka Sterle[2] · Franci Pušavec[2] · Miha Čekada[1]

Received: 15 January 2026 / Accepted: 3 April 2026

Abstract
With the growing demand for sustainable manufacturing solutions, liquid carbon dioxide (LCO_2) has emerged as a promising alternative to conventional cooling lubricating fluids due to its environmentally friendly properties, non-toxicity, and high cooling capacity. This study investigates the influence of LCO_2 flow rate on the performance of TiAlN-coated cutting inserts during the turning of 42CrMo4 (AISI 4140) steel. Tool life, cutting forces, temperature, and surface roughness were evaluated at various LCO_2 flow rates. The results demonstrate that LCO_2 significantly affects machining performance. At optimal flow rates of 200–250 g/min, the tool life increases by up to 20% compared to dry cutting. Excessive LCO_2 flow reduces cooling effectiveness, leading to reduced tool life. At LCO_2 flow rates above 400 g/min, the tool life is even shorter compared to dry turning. Moreover, higher flow rates increase the machining costs without providing additional performance benefits. Although no changes in dominant wear mechanisms were observed when using LCO_2, its cooling effect clearly influences wear progression. Optimized flow rates slow down wear development, whereas excessive cooling of the workpiece can accelerate tool wear. These findings highlight the importance of optimizing the LCO_2 flow rate to achieve improved tool life, stable machining conditions, and cost-effective sustainable manufacturing.

Keywords Cryogenic machining · 42CrMo4 · TiAlN · Liquid carbon dioxide

1 Introduction

During metal cutting processes, heat is generated primarily at the tool–chip interface [1]. This results from severe plastic deformation during the chip formation and friction between the flowing chip and the rake face of the cutting tool [2, 3]. The generated heat is distributed among the tool, chip, and workpiece, influencing tool wear, surface integrity, and chip formation mechanisms [4, 5]. The extent of heat generation and its partitioning depend strongly on process parameters such as cutting speed, feed rate, and depth of cut, as well as on the cooling-lubrication conditions and thermo-mechanical properties of both the workpiece and tool materials [6, 7].

In dry machining, the thermal and tribo-mechanical loads on the cutting edge are typically mitigated by applying hard protective coatings. Among these, physical vapour deposition (PVD) coatings based on titanium aluminium nitride (TiAlN) are widely used. TiAlN coatings provide high hardness, excellent thermal stability and oxidation resistance, and retain favourable mechanical properties even at elevated temperatures [8, 9].

An alternative strategy for managing the thermal load is the use of cooling lubricating fluids (CLFs) [10]. These fluids reduce the coefficient of friction at the tool–chip and tool–workpiece interfaces and promote convective heat dissipation, thereby lowering the cutting temperature [11, 12]. However, elevated temperatures have a dual effect: while they soften the workpiece material and reduce cutting forces, they also deteriorate the mechanical properties of the tool and accelerate wear mechanisms such as diffusion and oxidation [13, 14]. Effective process control therefore requires maintaining the cutting temperature within an optimal range to balance these competing effects [15]. Conventional

✉ Matej Drobnič
matej.drobnic@ijs.si

[1] Department of Thin Films and Surfaces, Jožef Stefan Institute, Jamova 39, 1000 Ljubljana, Slovenia

[2] Faculty of Mechanical Engineering, Laboratory for Machining, University of Ljubljana, Aškerčeva 6, 1000 Ljubljana, Slovenia

Published online: 17 April 2026

cooling and lubrication are often achieved using oils or emulsions, applied in flood mode (typically < 2–3 bar) or in high-pressure mode (20–70 bar), but in neither case is the fluid delivery rate precisely controlled [16, 17]. More precise adjustment of cooling capacity by controlling the flow of the CLFs can be achieved using cryogenic media such as liquid nitrogen (LN_2) or liquid carbon dioxide (LCO_2). Compared with conventional CLFs, these cryogenic agents provide superior cooling performance and reduced environmental impact [11, 18]. After cutting, they evaporate and leave no residue, unlike other CLFs [19, 20]. Due to the use of cryogenic media, the tool also undergoes a form of cryogenic thermal treatment, which can improve its wear resistance and extend tool life; however, the effectiveness of this treatment strongly depends on the tool material and its microstructural response to deep cooling [21, 22].

The use of LN_2 is complicated by its extremely low storage temperature, requires insulation on the supply line, and is therefore not suitable for feeding through the spindle or turret of a machine tool, and does not allow mixing with oils. In contrast, LCO_2 offers a more practical alternative. It can be stored at room temperature in a gas cylinder, allowing straightforward handling and supply to the cutting zone in pure form or as a mixture with oil [23]. Due to the phase transformation of LCO_2 from liquid to a gaseous state when exiting the nozzle, the cooling effect depends on the heat transfer rate and latent heat transfer rate, which is directly related to the LCO_2 flow rate [24, 25].

Several authors have reported on milling and turning studies using pure LCO_2 with various flow rates. In milling processes, the number of teeth or nozzles must also be considered when calculating the total LCO_2 flow rate, as the key data is the LCO_2 flow rate per nozzle or flow rate per cutting edge. Therefore, the values for milling are presented as LCO_2 flow per individual nozzle.

Sadik et al. [18] studied milling of Ti-6Al-4 V using PVD coated inserts with three different LCO_2 flow rates (75, 85 and 325 g/min) and found that higher LCO_2 flow rates significantly extended the tool life. Khanna, N. et al. [26] used a flow rate of 800 g/min per nozzle in end milling of glass fiber reinforced polymer, which resulted in an 80% reduction in the cutting zone temperature, a lower tool wear, a 5% reduction in the modulus of cutting force, and a reduced surface roughness compared to dry machining. Cordes et al. [27] achieved higher material removal rates (+ 72%) and a significant reduction in tool wear rate (–63%) when milling stainless steel 1.4962 with an LCO_2 flow rate of 33 g/min per nozzle. In several studies the authors did not report the exact LCO_2 flow rate used in experiments [19, 28].

Experiments were also conducted for turning, where LCO_2 is typically supplied through a single nozzle. Wang et al. [29] used an LCO_2 flow rate of 750 g/min to compare various feed rates and cutting speeds when turning cylindrical roller bearing inner rings with PCD inserts. Similarly, Llanos et al. [30] conducted experiments on hard turning of components for roller bearings using LCO_2 at a flow rate of 500 g/min. Test cases showed that LCO_2 can outperform conventional cutting fluids in sustainability and cost-effectiveness. Furthermore, Jamil et al. [31] reported that when turning Ti-6Al-4 V using LCO_2 at a flow rate of 350–450 g/min, the temperature was reduced by 62% compared to dry cutting, and LCO_2 also significantly reduced tool wear compared to other cooling modes.

Tool wear and tribological studies using LCO_2 were also conducted in a laboratory environment, on a pin-on-disc [32] and open tribometer apparatus [33, 34]. Courbon et al. [33] used a flow rate of 130 g/min, while one of us [34] used 200 g/min. In our previous work [32], the flow rate of LCO_2 used in tribotests was set to approximately 83 g/min.

Despite the demonstrated benefits of cryogenic cooling in machining, systematic studies combining cryogenic media with coated carbide tools remain limited as shown in a review of the existing literature. Furthermore, there is a lack of experimental data on the thermal conditions at the cutting edge under pure LCO_2 cooling and their relationship with tool wear and surface integrity. Therefore, the aim of this study is to investigate the performance of TiAlN-coated carbide inserts in longitudinal turning of 42CrMo4 alloy steel under cryogenic cooling with different LCO_2 flow rates to present a methodology for determining optimal conditions for machining using LCO_2. Specifically, the study focuses on (i) in-situ measurement of temperatures on the cutting edge, (ii) analysis of cutting forces, (iii) evaluation of tool wear mechanisms, and (iv) characterization of the resulting surface integrity.

Therefore, this work examines in more detail the influence of various flow rates of pure LCO_2 on cutting zone temperature, tool wear and the TiAlN coating during turning of 42CrMo4 steel.

To ensure clarity and consistency, the abbreviations of all parameters used in this study are listed in Table 1.

Table 1 List of abbreviations

Abbreviation	Description	Units
R_e	yield strength	N/mm^2
R_m	ultimate tensile strength	N/mm^2
a_p	depth of cut	mm
f	feed rate	mm/rev
v_c	cutting speed	m/min
VB	flank wear	µm
VB_{max}	maximum flank wear	µm
F_c	cutting force	N
F_f	feed force	N
F_p	passive force	N
R_a	arithmetic average roughness	µm

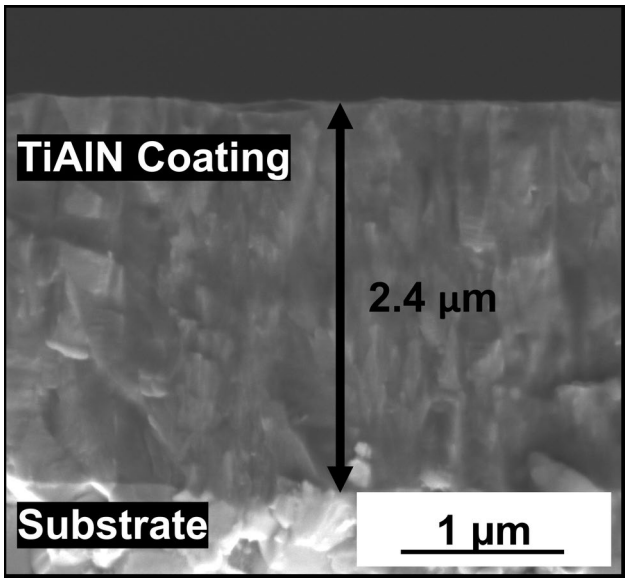

Fig. 1 SEM cross-sectional image of the TiAlN coating on the turning inserts

2 Experimental

2.1 Machining setup

Longitudinal turning experiments were conducted on a CNC lathe (Mori Seiki SL 153) using standardized tungsten carbide cutting inserts (DCMT11T304-MF2, Seco, Sweden) with a clearance angle of 7.0°, corner radius of 0.4 mm, cutting edge radius of 0.04 mm and an included angle of 55.0°. Before coating, all inserts were ultrasonically cleaned in ethanol and then sputter-etched to remove surface contaminants. A TiAlN coating was deposited in an industrial cathodic arc evaporation unit (Kobelco AIPocket) using TiAl targets with a Ti:Al atomic ratio of 40:60 (at.%). During the deposition process, the inserts were mounted in the holders with a three-fold rotation to promote uniform film growth [35, 36]. The resulting coating thickness was determined by cross-sectional scanning electron microscopy (SEM), yielding an average value of 2.4 µm (Fig. 1). Coating hardness was 29±3 GPa.

For tool temperature monitoring, blind holes of 0.6 mm diameter were manufactured into the inserts using electrical discharge machining (EDM, Makino EDA2F). Type K thermocouples (NiCr–Ni, Ø 0.4 mm, Class 1, IEC 584–2, temperature range: –40 to 1000 °C) were embedded in the machined holes so that the junction was positioned 0.4±0.01 mm beneath the rake surface as presented on Fig. 2c. Heat transfer was improved by using a copper paste between the thermocouple and the hole surface.

The tool holder was modified and upgraded with a custom 3D-printed nozzle to provide an internal LCO_2 delivery channel as close to the cutting edge as possible for effective cooling (Fig. 2b). The distance between the nozzle and the tip of the cutting insert was 7.65 mm (inset, Fig. 2a). This configuration enabled a direct supply of LCO_2 into the cutting zone during machining (Fig. 2a). The purity of applied LCO_2 used as the cryogenic coolant was≥99.5%. LCO_2 was stored in a gas cylinder and delivered at a room temperature (23 °C) and a pressure of 57 bar. The flow rate was constant in each measurement, and the selected range of LCO_2 flows was from 0 to 450 g/min with a division of 50 g/min. It was regulated using a precision needle valve and continuously monitored. For flows up to 200 g/min, measurements were taken using a Bronkhorst mini Cori-Flow digital mass flow meter (W14-AAD-BB-0-S), while higher flow rates (>250 g/min) were monitored with an ArcLub One system which has a built-in Bronkhorst Mini Cori Flow M15 coriolis mass flow meter. During the experiments, the average relative humidity was 55%±10%, while the average ambient temperature was 23 °C.

2.2 Materials

The workpiece material used in the experiments was hot-rolled 42CrMo4 (EN 10083–3, W.-Nr. 1.7225) alloy steel, equivalent to AISI 4140 (ASTM A29) alloy steel, supplied

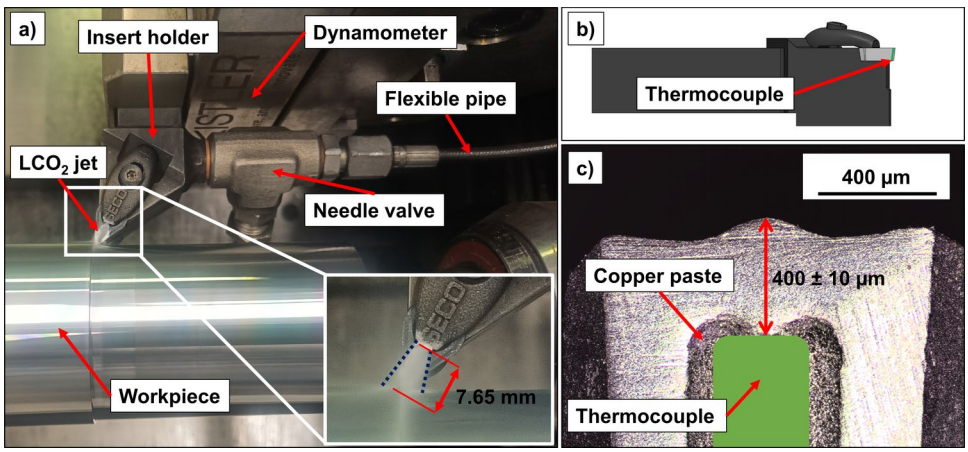

Fig. 2 Experimental setup (**a**) on the CNC lathe, cutting insert holder (**b**) with positioned thermocouple and cross-section of the cutting insert (**c**)

as round bars. It is widely used for highly loaded mechanical components where fatigue strength and toughness are critical [37].

However, its relatively high hardness and tensile strength, particularly in the quenched and tempered condition, result in elevated cutting forces, increased heat generation, and accelerated tool wear during machining. Chromium and molybdenum enhance hardenability and wear resistance but also increase abrasiveness and thermal load at the tool–chip interface. Consequently, machining of 42CrMo4 often presents challenges related to flank and crater wear, surface integrity alteration, and process stability [38, 39].

The bars were quenched at 860 °C ± 10 °C with a holding time of 5–7 h, followed by tempering at 560 °C ± 10 °C with a holding time of 7–9 h. The as-received bar diameter was 70 mm ± 1 mm. The nominal chemical composition is provided in Table 2. The mechanical properties of the heat-treated material were: yield strength (R_e) of 900 N/mm^2 and ultimate tensile strength (R_m) of 1025 N/mm^2.

Hardness was evaluated using Rockwell hardness test (OMAG 206 RT) on cross-sectional specimens taken from three bars. The results indicated a uniform hardness distribution across diameters between 38 and 68 mm (Fig. 3). Below 38 mm, a noticeable reduction in hardness was observed. Therefore, all machining tests were conducted within the 38–68 mm diameter range to ensure material uniformity and experimental repeatability. Preliminary experiments confirmed that this range provided consistent tool life, whereas smaller diameters exhibited a significantly extended tool life under identical cutting conditions. The measured hardness for the selected diameters was 35 ± 1 HRc. Before each experiment, a cleaning pass was performed on the bar surface to remove the outer layer and ensure an initial diameter of 68 mm.

The length of the workpieces was 330 mm in total, resulting in an effective machining length of 300 mm. Each workpiece was securely clamped at one end and supported by a tailstock at the opposite end to ensure stability during machining.

2.3 Methods

To select the optimal turning parameters, preliminary experiments were conducted to analyze the influence of cutting depth and cutting speed on tool life under dry conditions. The aim was to determine the appropriate parameters that would enable a time- and cost-effective study of the impact of LCO_2 on the turning process in the next step. Preliminary cutting speeds were selected based on the recommended machining parameters for these cutting inserts, in the range of 150–300 m/min with a division of 50 m/min. Depth of cut (a_p) used for preliminary experiments was 1 mm and 1.5 mm.

Based on the results of preliminary experiments shown in Fig. 4, we selected the cutting speeds and cutting depths (shaded area) that were used for further research. The selected turning parameters enabled a comparison between different conditions, while the maximum turning length was suitable for the experimental setup. The cutting parameters were kept constant, with a depth of cut (a_p) of 1 mm and a feed rate (f) of 0.2 mm/rev. Two cutting speeds (v_c) were selected: 250 and 300 m/min. We focused on higher cutting speeds also to increase productivity, which is one of the purposes of using LCO_2 [40, 41].

The LCO_2 supply was opened and allowed to stabilize just before the tool came into contact with the workpiece. This stabilization took a few seconds, as the liquid phase needed to reach the nozzle. As a result, the tool was briefly exposed to cryogenic heat treatment, an effect that is unavoidable due to the nature of the LCO_2 supply method [42, 43]. Potential deviations arising from these factors were minimized by repeating the experiments multiple times. Additionally, the impact of cryogenic treatment was mitigated by the selection of the tool material, which affects WC–Co to a lesser extent than, for example, HSS [21, 44, 45]. Since the cutting

Table 2 Chemical composition of the 42CrMo4 alloy steel used for the study

C	P	Ni	Cu	Si	S	Mo	Mn	Cr	Al
0.4	0.014	0.03	0.02	0.2	0.026	0.16	0.74	1.03	0.025

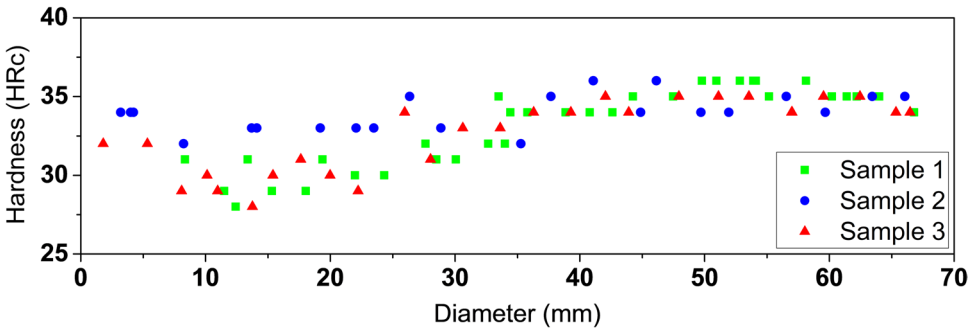

Fig. 3 Hardness of the 42CrMo4 alloy steel across the bar cross-section

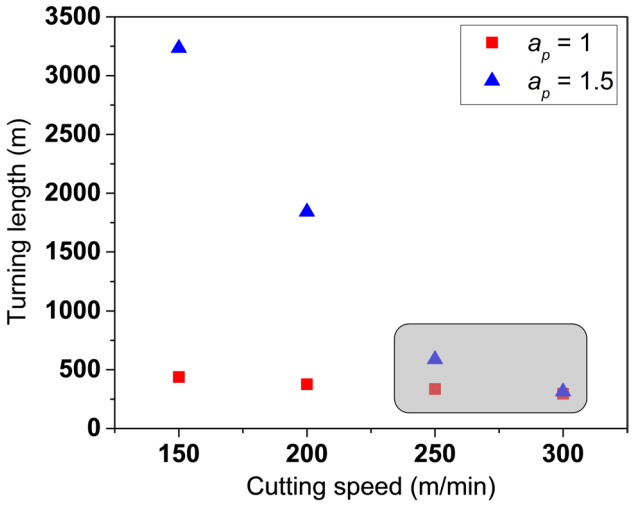

Fig. 4 Turning length (in m) versus cutting speed (in m/min) for $a_p = 1$ and $a_p = 1.5$. The shaded area indicates the selected cutting speeds used in this study

insert tool life exceeded the length of a single pass, the experiment was performed on the same workpiece in several passes, at different diameters. The tool moved to the initial turning position using a rapid feed, with the LCO_2 supply maintained constant throughout. At different machining lengths with different number of passes no deviations were observed attributable to the brief exposure of the tool to LCO_2 while it was not in contact with the workpiece.

Cutting forces were recorded using a piezoelectric dynamometer (Kistler, type 9129AA). Surface roughness of the machined workpieces was measured with a portable profilometer (Mitutoyo Surftest SJ-301). Tool wear and wear mechanisms were characterized by scanning electron microscopy (SEM, Thermo Fisher Quanta 650 ESEM and Helios Nanolab 650).

3 Results and discussion

3.1 Tool life

The flank wear *VB* of cutting tools is often chosen as a tool life criterion, as it directly affects the machining accuracy, stability and reliability of the process [46]. Under dry (Fig. 5a) and LCO_2 (Fig. 5b) cutting conditions, the flank wear was stable, but at the end of the tool life, wear increased rapidly, so monitoring wear at individual time intervals was not appropriate. Furthermore, crater wear was present, which also caused tool breakage. While it is possible to measure wear on the flank face only at selected intervals, indirect real-time wear monitoring is also possible by monitoring cutting forces, which reflect the gradual development of the wear [47]. Therefore, we chose a rapid increase in cutting forces just before the tool failure as the wear criterion, which coincides with the increased flank wear over the wear criterion, as shown in Fig. 5. However, not all cutting forces increase equally with increasing wear, radial/axial components (passive and feed force) are more sensitive than the main cutting force [48]. We therefore determined the wear criterion as when one of the forces increases by more than 20% in a time of < 5 s which also indicates accelerated wear near VB_{max}.

The relation between the tool life and the LCO_2 flow rate at cutting speeds of 250 m/min and 300 m/min using turning inserts with TiAlN and without coating is shown in Fig. 6. The measurements were repeated at least three times to ensure repeatability. The error bars represent the standard deviation, reaching up to 11% for TiAlN-coated tools and up to 20% for uncoated tools.

The uncoated inserts were used for comparison only, so measurements were made using LCO_2 at flow rates

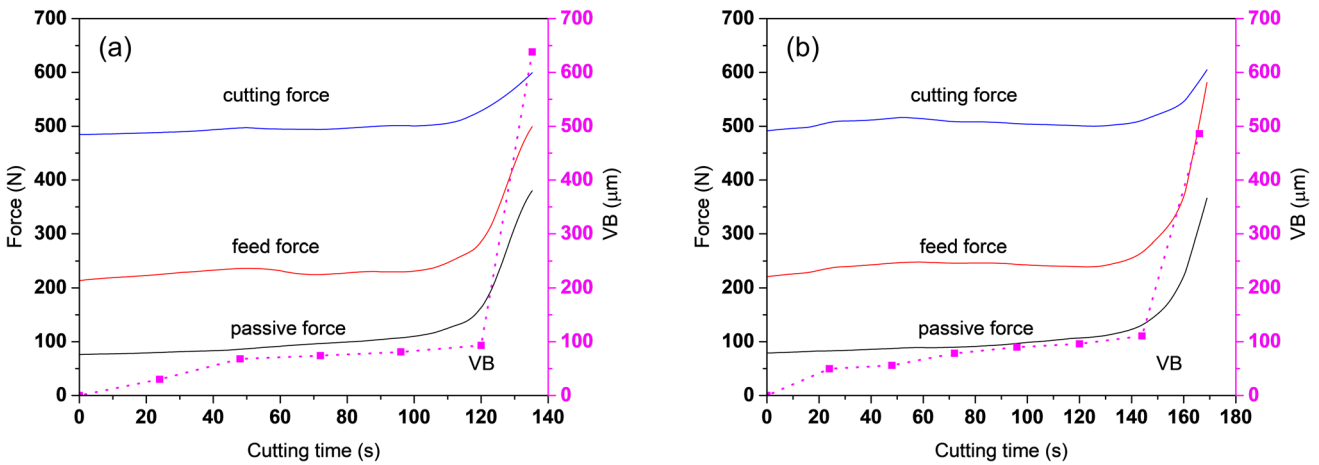

Fig. 5 Correlation between cutting forces and wear VB at cutting speed of 250 m/min in dry cutting mode (**a**) and with LCO_2 flow of 200 g/min (**b**)

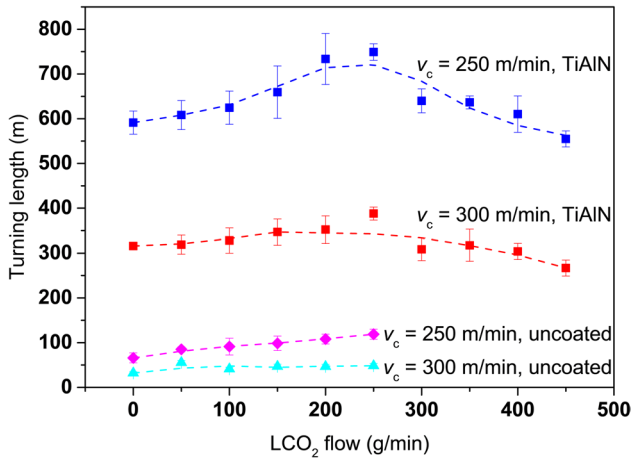

Fig. 6 Turning length versus LCO_2 flow rate for uncoated and TiAlN coated inserts at cutting speeds of 250 and 300 m/min. Error bars represent standard deviation

of 0–250 g/min. The lowest tool life was at dry cutting conditions and prolonged with LCO_2 flow. At a cutting speed of 250 m/min, the tool life prolonged by ≈180% with LCO_2, and by ≈170% at 300 m/min. TiAlN coated inserts had a significantly longer tool life compared to uncoated tools, and the difference between dry and LCO_2 assisted cutting was also more intense. When using LCO_2 at cutting speed of 250 m/min, the TiAlN coated tool had a 6–9 times longer tool life compared to the uncoated inserts. Similar, at cutting speed of 300 m/min, the tool life is prolonged by a factor of 6–10 compared to the uncoated tools at the same cutting speed. At both cutting speeds, the tool life of TiAlN coated inserts reaches its peak at 200–250 g/min LCO_2. As the LCO_2 flow rate increases further, the tool life begins to decline and above 400 g/min it even reaches values lower than at the dry cutting mode.

3.2 Temperature

In order to understand the influence of LCO_2 flow on tool life, it is also necessary to consider the temperature conditions during cutting. Although we did not measure the temperature exactly in the cutting zone at the tool/workpiece/chip interface, we can compare individual temperature conditions from the temperature measurements under the tool surface. It should be noted that the temperature at the actual tool–chip interface cannot be measured directly in practice and can only be estimated using FEM method [49, 50], which is beyond the scope of the present study. Instead, our approach relies on previously published studies [51–53] where temperatures were determined using various experimental methods, including the placement of thermocouples just below the surface of the cutting insert.

Figure 7a shows temperature measurements at the beginning, middle and end of turning at a cutting speed of 250 m/min, and Fig. 7b at a cutting speed of 300 m/min. Comparison of the values in three different turning phases confirms the increase in temperature with wear. The more the cutting edge is worn, the greater the friction and the higher the temperatures, which is also confirmed by other studies [54, 55]. Under dry cutting conditions at a cutting speed of 250 m/min the temperature increases by up to 25%, whereas at 300 m/min, the increase is smaller, approximately 10%. When comparing different LCO_2 flows, we found that temperatures decrease with increasing flow of LCO_2. However, at a cutting speed of 250 m/min, the temperature is constant at flow rates from 250 g/min onwards, and at a cutting speed of 300 m/min it is constant from 300 g/min onwards. These values indicate that the temperature in the cutting zone does not depend linearly on the LCO_2 flow rate. LCO_2 lowers the temperature

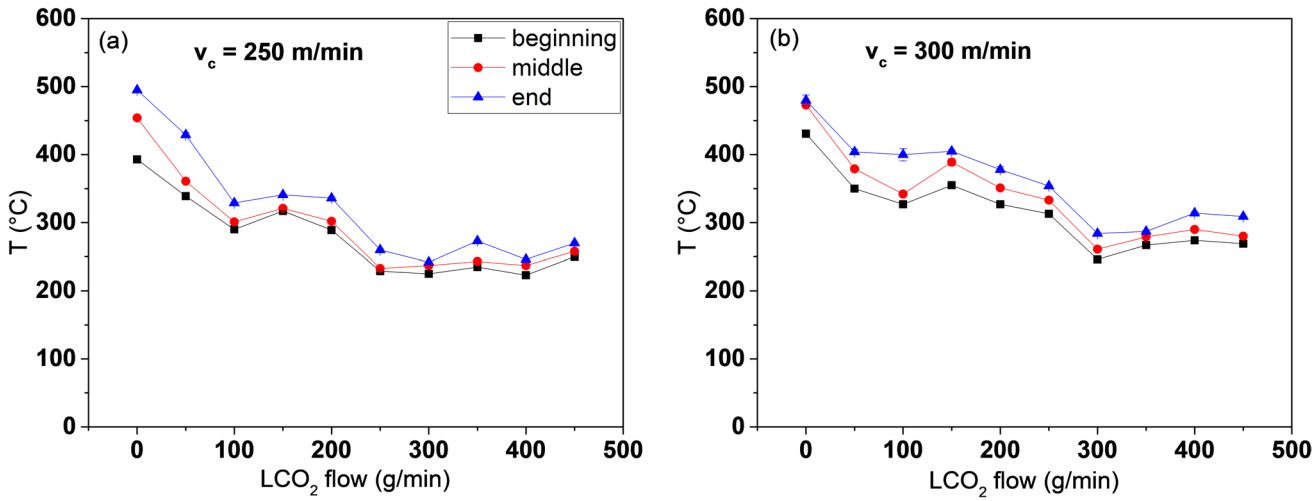

Fig. 7 Temperature in various stages measured 0.4 mm under the turning insert surface at cutting speeds of 250 m/min (**a**) and 300 m/min (**b**)

due to the cooling effect [56], but this cooling effect is limited. The reason may also lie in the design of the cutting setup itself, especially the distance between the nozzle and the cutting zone and shape of the nozzle [57].

Given the increased tool wear at LCO_2 flows above 250 g/min and the stationary temperature conditions in the tool at these flows, it is also likely that a higher LCO_2 flow does not only remove heat from the tool, but rather increases heat dissipation from the workpiece and tool material. As a result, the softening of the material due to increased temperatures is less pronounced, which consequently promotes tool wear, especially abrasion and the associated crater wear.

3.3 Cutting forces

We measured the cutting (tangential, F_c), feed (axial, F_f) and passive (radial, F_p) forces using a piezoelectric dynamometer. The measured values show that the main cutting force is the largest, followed by the feed force and the passive force is the smallest. All three cutting force components increase with wear, similar as temperature, as shown in Fig. 5, and for the force comparison we therefore chose the average values of the individual sections. Figure 8 shows the force values at the beginning, middle and end of turning. For better visualization, a linear fit is also added to the values, showing the trend of the force magnitude depending on the LCO_2 flow.

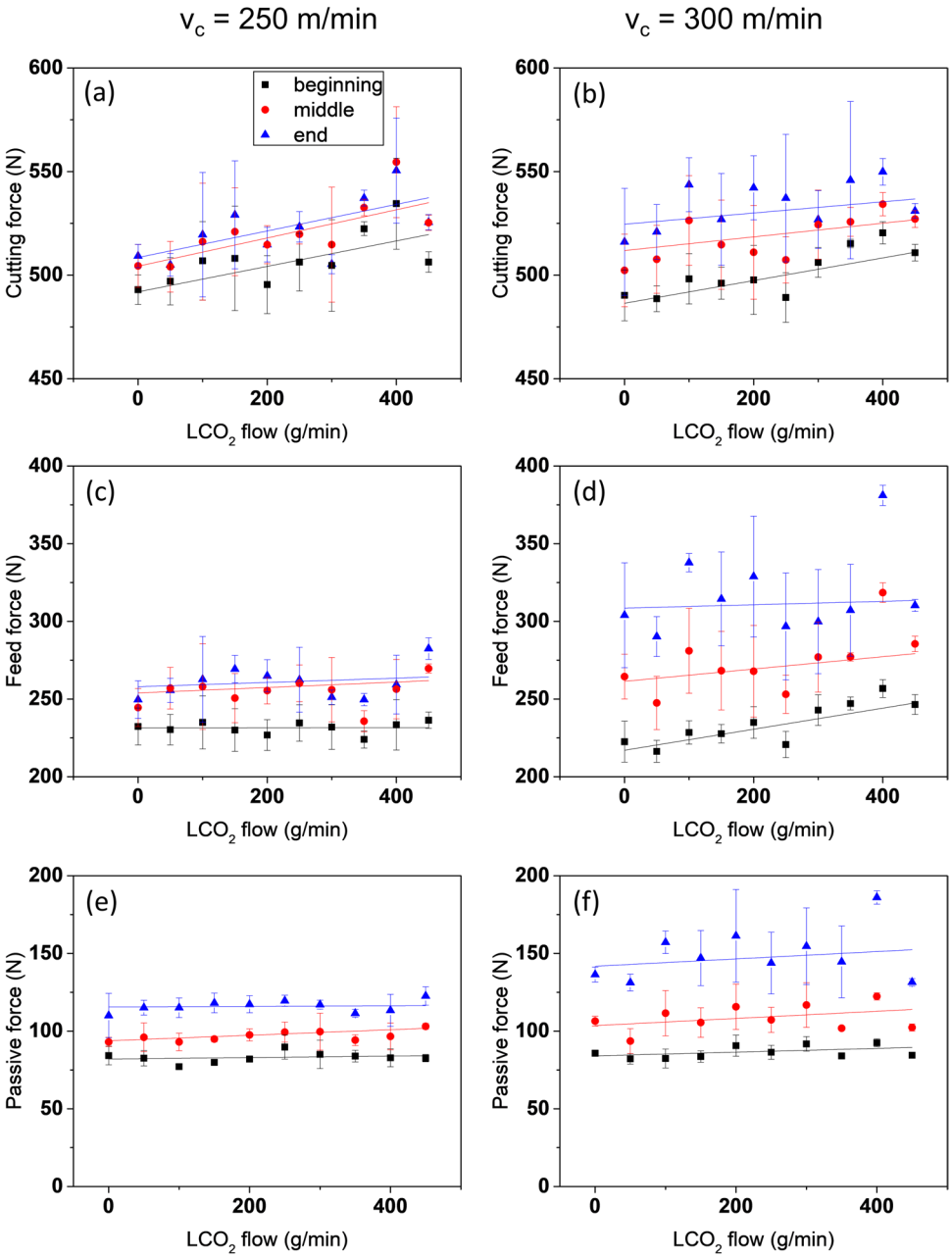

Fig. 8 Cutting force (**a**, **b**), feed force (**c**, **d**) and passive force (**e**, **f**) at cutting speeds of 250 m/min (**a**, **c**, **e**) and 300 m/min (**b**, **d**, **f**) at various LCO_2 flow rates

Similar to the temperature, the forces also increase with increasing wear, which confirms the correlation between the cutting forces, wear and temperature in the cutting zone [58]. A higher LCO_2 flow allows more heat to be removed, but the distribution is probably no longer effective enough to cool only the tool, but also the workpiece, which in turn affects the increase in cutting forces. Therefore, in addition to the LCO_2 flow rate, the number, orientation and shape of the supply nozzles are also important to enable a precise cooling of only the tool without the surrounding area.

The main cutting force is presented in Fig. 8a for v_c=250 m/min and in Fig. 8b for v_c=300 m/min remained consistently in the range of 500–550 N across all LCO_2 flow rates and at both cutting speeds. The values show no statistical differences between both cutting speeds, however, cutting forces increase with LCO_2 flow. The greater increase in cutting forces with LCO_2 flow at 250 m/min compared to 300 m/min can be explained by the better cooling effect of the workpiece material at lower cutting speeds, since due to the workpiece rotation speed, the material is in contact with LCO_2 for a longer time and therefore undergoes stronger cooling. Due to lower temperatures, there is less temperature-related material softening, which increases the cutting forces.

Conversely, no significant differences were observed in the feed and passive forces between the various LCO_2 flow rates. At a cutting speed of 250 m/min, the feed forces at the beginning and in the middle of the turning process were similar to those at 300 m/min, ranging from 220–250 N at the start and 230–280 N in the middle. At the end, however, the feed forces at 300 m/min were approximately 25% higher than those at 250 m/min which remained within the range measured in the middle of the cut. The same is observed for the passive force which is in the range of 80–120 N at the cutting speed of 250 m/min and in the range of 80–170 N at the cutting speed of 300 m/min. It can be concluded, as also evident from the graphs, that both the feed and passive forces do not vary with the LCO_2 flow rate.

3.4 Wear mechanisms

The measured workpiece surface roughness value (R_a) during initial and steady wear stage was similar for all parameters – at a speed of 250 m/min R_a was 3.33±0.15 µm and at a speed of 300 m/min it was 3.32±0.14 µm. No difference was observed in surface roughness between different LCO_2 flows including dry cutting. Given that the machining parameters and the choice of the cutting inserts are suitable for medium machining, it is not expected that the roughness of the machined surface of the workpiece will change significantly [59].

Tool wear analysis was performed using SEM on all rake and flank faces of the used cutting inserts. Similar tool wear modes were observed in both, dry and LCO_2 assisted turning. On the rake face (see Fig. 9a and c) crater wear, Build-Up-Edge (BUE) and Build-Up-Layer (BUL) are the main wear modes while on the flank face (see Fig. 10a and c) the main wear modes observed are adhesion of the workpiece material and formation of micro cracks. Crater wear first begins to form on the chip breaker in the initial wear stage and only fully develops in the last phase of the turning in the rapid wear stage [60]. During the steady stage the wear remains similar to the initial stage and does not increase significantly. Crater wear occurs as a result of chip abrasion, which is also confirmed by abrasive traces perpendicular to the tool feed direction, as shown in Fig. 9b [61].

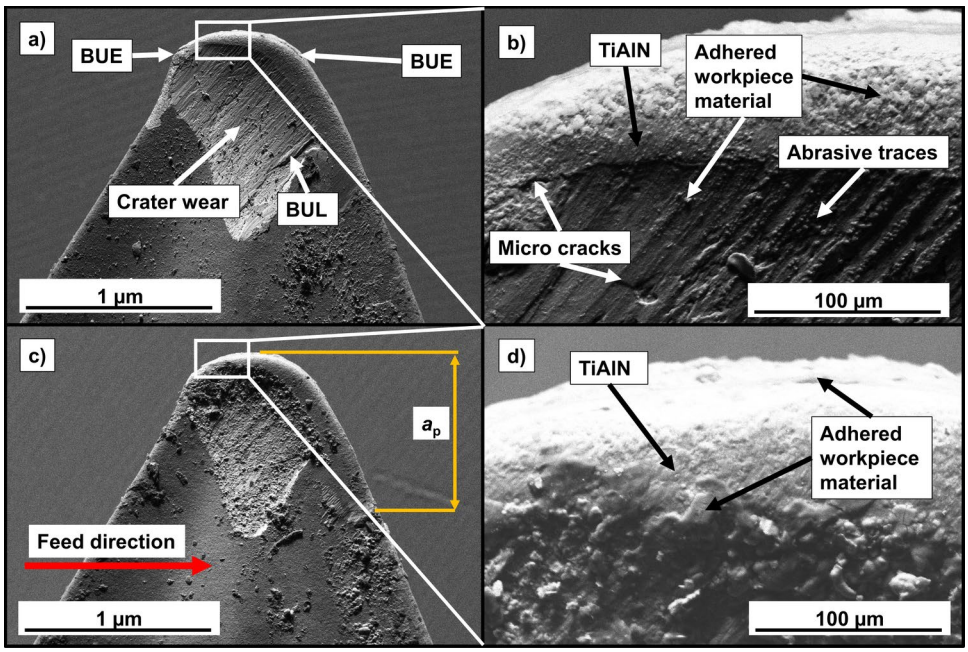

Fig. 9 Rake face of the cutting insert after turning at 250 m/min in dry cutting mode (**a**, **b**) and with LCO_2 flow of 200 g/min (**c**, **d**). The main types of wear are crater wear and adhesion of material on the cutting edge

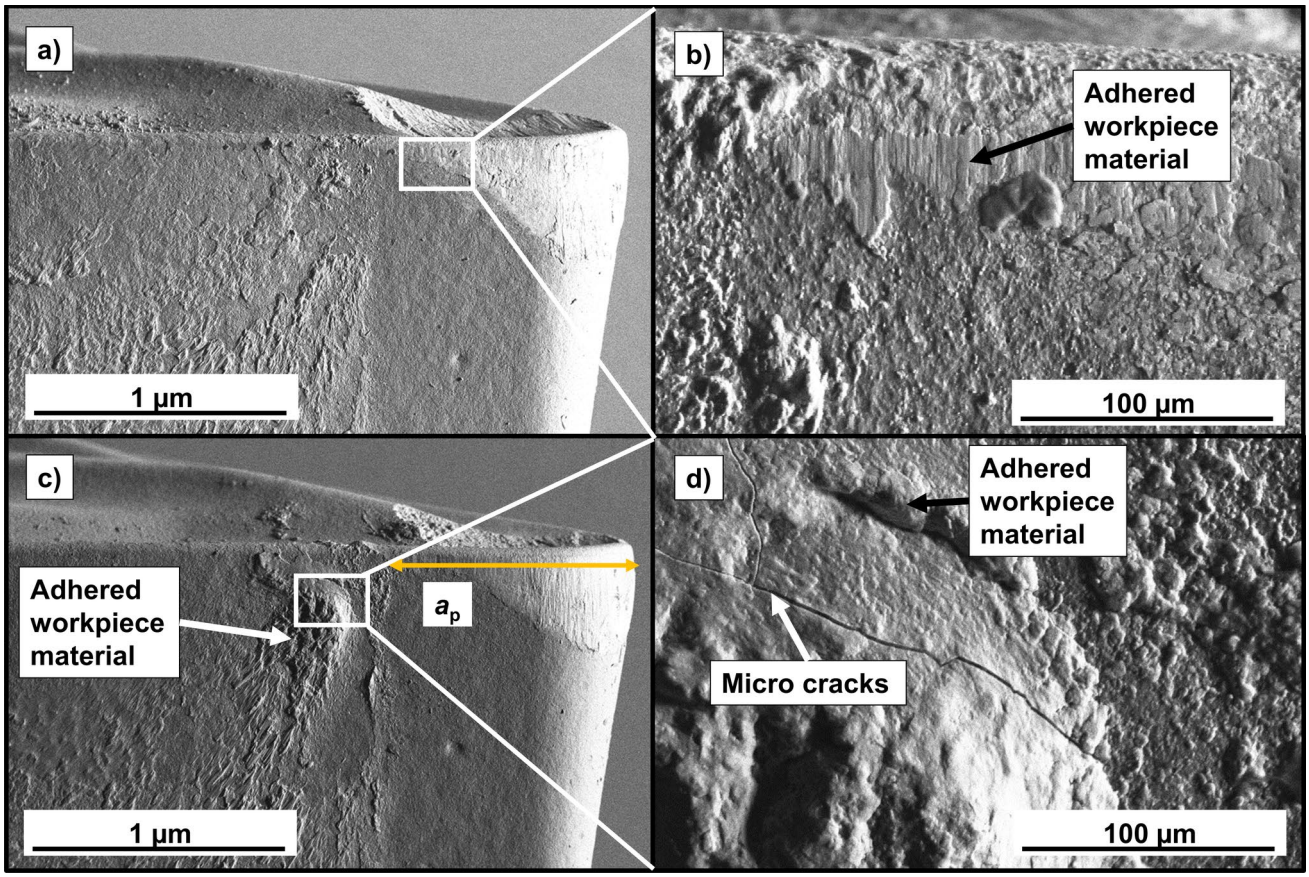

Fig. 10 Flank face of the cutting insert after turning at 250 m/min in dry cutting mode (**a**, **b**) and with LCO_2 flow of 200 g/min (**c**, **d**)

On the rake face, abrasion causes initial crater wear on the hard coating, while directly on the cutting edge the hard coating remains and the workpiece material adheres to it. The chip is formed on the cutting edge and only changes its direction of movement at the chip breaker, which is why the temperature on the cutting insert is the highest slightly above the cutting edge on the rake face as a result of friction between the chip and the rake face [62]. However, material adhesion occurs at the cutting edge which is clearly visible from SEM and EDS analyses. When using LCO_2, it is expected that adhesion will be less intensive due to better cooling and poorer thermal softening of the workpiece material [10]. This is true to a certain extent, but adhesion is still present, which is visible from the analyses.

With increased LCO_2 flows the wear mechanisms are similar (Fig. 9d and Fig. 10d). The temperature graphs (Fig. 7) indicate that from LCO_2 flow rate of 250 or 300 g/min onwards the measured temperature in the cutting insert is similar. This means that a larger amount of LCO_2 does not cause a lower temperature, as the maximum cooling occurs at a flow rate of 250 g/min. Anything above this amount only causes even more active cooling of the surroundings. Despite active cooling, heat generation is still high enough to partially soften the material, resulting in the formation of BUE and BUL. Due to the adhered material, the radius of the cutting edge increases and the geometry of the tool changes, which affects the formation of chips, and above all, increases the cutting forces [63]. Friction and heat generation also increase. With increasing cutting forces, crater wear also increases, which weakens the cutting edge [60]. The weakened cutting edge and increased cutting forces, together with the micro cracks, cause tool breakage. Although higher LCO_2 flows reduce the formation of BUE, they also reduce the softening of the workpiece material, which results in higher cutting forces, which, according to our results, has a greater impact on tool wear than the increase in forces due to BUE formation.

The depth of cut a_p is clearly visible from the flank face, where the surface is smooth without adhered material (Fig. 10a and c). However, material deposition is noticeable on the areas of the cutting insert that are not in the a_p area (Fig. 10d). On the worn surface of the flank face, particles of workpiece material are adhered to the TiAlN coating and then peeled off, causing adhesive wear. At the cutting speed of 250 m/min, the flake with adhered workpiece material is clearly visible on all cutting inserts. In contrast, on cutting inserts that were used for turning at 300 m/min, there is less visible adhered material on the flank face.

At both cutting speeds, the adhered material (BUL) on the flank face has visible cracks (Fig. 10d). This suggests that when the layer of adhered material becomes thick enough, it peels off the surface, removing part of the coating and causing adhesion wear, as shown in Fig. 11. Grooves are also visible on the coating indicating the abrasion wear.

At higher LCO_2 flow rates (300 g/min and above) a greater amount of adhered material was observed on the flank face than at lower LCO_2 flow rates, indicating that the larger amount of LCO_2 carried away more micro particles of the workpiece material at a time, and due to the LCO_2 flow, the material was also deposited on the part of the flank face that was not in contact with the workpiece. Due to the higher cutting forces, there were also higher contact pressures which caused increased wear and faster material fatigue.

A higher LCO_2 flow would enable even more intense heat removal, but due to the limited heat transfer rate, this heat would not be removed only from the tool or cutting zone, but from the workpiece material and the surroundings, since the cooling capacity of LCO_2 per area unit is limited. Using the cutting parameters selected in this study, heat generation is larger than what can be removed by using LCO_2 from the cutting area. The cooling effect with LCO_2 would therefore probably increase with increasing a_p and decreasing cutting speeds, which is also consistent with our observations. At lower cutting speeds, we can cool the tool in the cutting zone more effectively, without cooling the workpiece material, and thus prevent thermal softening, which results in lower cutting forces and lower wear. This can therefore be achieved by knowing the optimal cutting temperature and, above all, by using a precise cooling method, which LCO_2 enables. In addition to increasing wear, using a too high flow of LCO_2 also makes no sense from an economic point of view, as it also significantly affects the machining costs [64]. Furthermore, for precise cooling, it makes sense to position the supply nozzles so that the largest possible portion of the LCO_2 flow is directed into the area of highest temperatures on the cutting insert, which are on the rake face, slightly away from the cutting edge [65, 66].

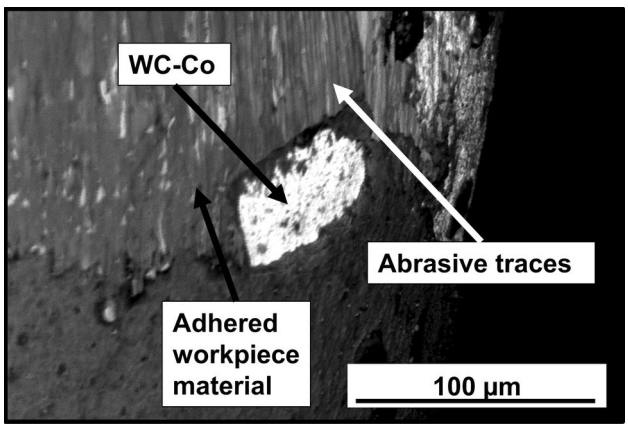

Fig. 11 Adhesive wear on the flank face of the cutting insert (v_c = 250 m/min, LCO_2 flow rate = 400 g/min). In addition to the adhesion (workpiece material), a part of the coating is also peeled off

4 Conclusions

In this study, we compared the wear of TiAlN-coated cutting inserts for turning of 42CrMo4 (AISI 4140) steel using various LCO_2 flow rates. The wear rate depends both on the cutting parameters and the workpiece material; therefore, we selected parameters that enabled a comparison between various LCO_2 flow rates, while ensuring the expected turning length was sufficient for the experiments. The experiments were conducted using bar diameters that ensured reproducibility of the results. We found the following:

- The use of TiAlN coating increases tool life up to a factor of 9 at the cutting speed of 250 m/min and up to a factor of 10 at 300 m/min compared to the uncoated tool.
- The turning length strongly depends on the cutting parameters. At v_c = 300 m/min, the turning length is reduced by 50% compared to v_c = 250 m/min in dry cutting.
- Tool life depends on the LCO_2 flow rate; at flow rates of 200–250 g/min, the tool life increases by up to 20% compared to dry cutting, while at higher LCO_2 flow rates, it begins to decrease and at LCO_2 flow rates above 400 g/min, it is even shorter than when turning without LCO_2.
- The temperature at the tip of the cutting insert increases with wear. At higher cutting speeds, higher cutting temperatures are also reached. The temperature also depends on the amount of LCO_2 used, with temperatures decreasing up to a flow rate of 250 g/min LCO_2, and then not changing significantly with further increasing of the LCO_2 flow. Compared to dry turning, the LCO_2 flow reduced temperatures by up to 50%.
- Turning forces increase with tool wear. The passive and feed forces do not change noticeably with the supply of LCO_2 to the cutting zone, regardless of the flow rate. In contrast, the cutting force increases with increasing LCO_2 flow rate, by up to 25%. It is therefore suggested to position the supply nozzles so that the largest possible proportion of the LCO_2 flow is directed into the area of highest temperatures on the cutting insert.
- At the selected cutting parameters using LCO_2, the main type of observed wear was crater wear on the rake face. The main wear mechanism on the flank face was

adhesion wear. Although we did not observe any changes in wear mechanisms when using LCO_2, it slows them down due to its cooling effect, or if the workpiece material is cooled too much, it even accelerates them.

Author contributions All authors contributed to the study conception and design. Material preparation, data collection and analysis were performed by Matej Drobnič, Luka Sterle and Miha Čekada. The first draft of the manuscript was written by Matej Drobnič and all authors commented on previous versions of the manuscript. All authors read and approved the final manuscript.

Funding This research was financially supported by the Slovenian Research and Innovation Agency (ARIS) within the framework of Young Researcher program and research core funding program P2-0082.

Declarations

Competing interests The authors have no relevant financial or non-financial interests to disclose.

References

1. Stephenson DA, Agapiou JS (2006) Metal Cutting Theory and Practice, 2 nd. CRC Press Taylor and Francis group, Boca Raton
2. Ogedengbe TS, Okediji AP, Yussouf AA, et al (2019) The Effects of Heat Generation on Cutting Tool and Machined Workpiece. J Phys Conf Ser 1378. https://doi.org/10.1088/1742-6596/1378/2/022012
3. Ay H, Yang WJ (1998) Heat transfer and life of metal cutting tools in turning. Int J Heat Mass Transf 41:613–623. https://doi.org/10.1016/S0017-9310(97)00105-1
4. Abukhshim NA, Mativenga PT, Sheikh MA (2006) Heat generation and temperature prediction in metal cutting: a review and implications for high speed machining. Int J Mach Tools Manuf 46:782–800. https://doi.org/10.1016/j.ijmachtools.2005.07.024
5. Stephenson DA, Ali A (1992) Tool temperatures in interrupted metal cutting. J Eng Ind 114:127–136. https://doi.org/10.1115/1.2899765
6. Young HT (1996) Cutting temperature responses to flank wear. Wear 201:117–120. https://doi.org/10.1016/S0043-1648(96)07227-4
7. Wright PK, McCormick SP, Miller TR (1980) Effect of rake face design on cutting tool temperature distributions. J Eng Ind 102:123–128. https://doi.org/10.1115/1.3183843
8. Koller CM, Hollerweger R, Sabitzer C et al (2014) Thermal stability and oxidation resistance of arc evaporated TiAlN, TaAlN, TiAlTaN, and TiAlN/TaAlN coatings. Surf Coatings Technol 259:599–607. https://doi.org/10.1016/j.surfcoat.2014.10.024
9. Bartosik M, Rumeau C, Hahn R, et al (2017) Fracture toughness and structural evolution in the TiAlN system upon annealing. Sci Reports 2017 71 7:1–9. https://doi.org/10.1038/s41598-017-16751-1
10. Proud L, Tapoglou N, Slatter T (2022) A Review of CO2 Coolants for Sustainable Machining. Metals (Basel) 12. https://doi.org/10.3390/met12020283
11. Ravi S, Gurusamy P, Mohanavel V (2021) A review and assessment of effect of cutting fluids. Mater Today Proc 37:220–222. https://doi.org/10.1016/j.matpr.2020.05.054
12. Liu H, Meurer M, Bergs T (2025) Comparative analysis of emulsion, cutting oil, and synthetic oil-free fluids on machining temperatures and performance in side milling of Ti-6Al-4V. Lubricants 13(9):396. https://doi.org/10.3390/lubricants13090396
13. Wan W, Zhou QG, Liang M et al (2024) Study on the high temperature wear behavior of TiAlSiN coatings deposited on WC-TaC-Co cemented carbides. Tribol Int 200:110115. https://doi.org/10.1016/j.triboint.2024.110115
14. Moghaddam PV, Prakash B, Vuorinen E et al (2021) High temperature tribology of TiAlN PVD coating sliding against 316L stainless steel and carbide-free bainitic steel. Tribol Int 159:106847. https://doi.org/10.1016/j.triboint.2020.106847
15. Pimenov DY, Der O, Manjunath Patel GC et al (2025) State-of-the-art review of energy consumption in machining operations: challenges and trends. Renew Sustain Energy Rev 224:116073. https://doi.org/10.1016/j.rser.2025.116073
16. Kui GWA, Islam S, Reddy MM et al (2021) Recent progress and evolution of coolant usages in conventional machining methods: a comprehensive review. Int J Adv Manuf Technol. https://doi.org/10.1007/S00170-021-08182-0
17. Cica D, Kramar D (2023) Machinability investigation and sustainability analysis of high-pressure coolant assisted turning of the nickel-based superalloy Inconel 718. Proc Inst Mech Eng Part B J Eng Manuf 237:43–54. https://doi.org/10.1177/09544054221092939
18. Sadik MI, Isakson S, Malakizadi A, Nyborg L (2016) Influence of coolant flow rate on tool life and wear development in cryogenic and wet milling of Ti-6Al-4V. Procedia CIRP 46:91–94. https://doi.org/10.1016/j.procir.2016.02.014
19. Nimel Sworna Ross K, Ganesh M (2019) Performance Analysis of Machining Ti–6Al–4V Under Cryogenic CO2 Using PVD-TiN Coated Tool. J Fail Anal Prev 19:821–831. https://doi.org/10.1007/s11668-019-00667-1
20. Benedicto E, Carou D, Rubio EM (2017) Technical, economic and environmental review of the lubrication/cooling systems used in machining processes. Procedia Eng 184:99–116. https://doi.org/10.1016/j.proeng.2017.04.075
21. Adin MŞ (2024) Machining aerospace aluminium alloy with cryo-treated and untreated HSS cutting tools. Adv Mater Process Technol 10:2664–2689. https://doi.org/10.1080/2374068X.2023.2273035
22. Kalsi NS, Sehgal R, Sharma VS (2010) Cryogenic treatment of tool materials: a review. Mater Manuf Process 25:1077–1100. https://doi.org/10.1080/10426911003720862
23. Bergs T, Pusavec F, Koch M et al (2019) Investigation of the solubility of liquid CO2 and liquid oil to realize an internal single channel supply in milling of Ti6Al4V. Procedia Manuf 33:200–207. https://doi.org/10.1016/j.promfg.2019.04.024
24. Pusavec F, Lu T, Courbon C et al (2016) Analysis of the influence of nitrogen phase and surface heat transfer coefficient on cryogenic machining performance. J Mater Process Technol 233:19–28. https://doi.org/10.1016/j.jmatprotec.2016.02.003
25. Busch K, Hochmuth C, Pause B, et al (2016) Investigation of Cooling and Lubrication Strategies for Machining High-temperature

Alloys. In: Procedia CIRP. Elsevier B.V., pp 835–840. https://doi.org/10.1016/j.procir.2015.10.005
26. Khanna N, Rodríguez A, Shah P et al (2022) Comparison of dry and liquid carbon dioxide cutting conditions based on machining performance and life cycle assessment for end milling GFRP. Int J Adv Manuf Technol 122:821–833. https://doi.org/10.1007/S00170-022-09843-4
27. Cordes S, Hübner F, Schaarschmidt T (2014) Next generation high performance cutting by use of carbon dioxide as cryogenics. In: Procedia CIRP. Elsevier, pp 401–405. https://doi.org/10.1016/j.procir.2014.03.091
28. Sadik MII, Isakson S (2017) The role of PVD coating and coolant nature in wear development and tool performance in cryogenic and wet milling of Ti-6Al-4V. Wear 386:204–210. https://doi.org/10.1016/j.wear.2017.02.049
29. Wang J, Zhang J, Peng R et al (2023) Research on cutting parameters of low-temperature liquid CO2 assisted PCD tool turning bearing ring. J Manuf Process 87:199–208. https://doi.org/10.1016/j.jmapro.2023.01.009
30. Llanos I, Urresti I, Bilbatua D, Zelaieta O (2023) Cryogenic CO2 assisted hard turning of AISI 52100 with robust CO2 delivery. J Manuf Process 98:254–264. https://doi.org/10.1016/j.jmapro.2023.05.036
31. Jamil M, He N, Zhao W et al (2021) Heat transfer efficiency of cryogenic-LN2 and CO2-snow and their application in the turning of Ti-6AL-4V. Int J Heat Mass Transf 166:120716. https://doi.org/10.1016/j.ijheatmasstransfer.2020.120716
32. Drobnič M, Drnovšek A, Pušavec F, Čekada M (2025) Effect of liquid CO2 on wear behaviour of TiAlN hard coating at elevated temperatures. Coatings 15(5):553. https://doi.org/10.3390/coatings15050553
33. Courbon C, Sterle L, Cici M, Pusavec F (2020) Tribological effect of lubricated liquid carbon dioxide on TiAl6V4 and AISI1045 under extreme contact conditions. Procedia Manuf 47:511–516. https://doi.org/10.1016/j.promfg.2020.04.139
34. Pušavec F, Sterle L, Kalin M et al (2020) Tribology of solid-lubricated liquid carbon dioxide assisted machining. CIRP Ann 69:69–72. https://doi.org/10.1016/j.cirp.2020.04.033
35. Panjan M, Čekada M, Panjan P et al (2007) Sputtering simulation of multilayer coatings in industrial PVD system with three-fold rotation. Vacuum 82:158–161. https://doi.org/10.1016/j.vacuum.2007.07.053
36. Panjan M (2013) Influence of substrate rotation and target arrangement on the periodicity and uniformity of layered coatings. Surf Coat Technol 235:32–44. https://doi.org/10.1016/j.surfcoat.2013.06.126
37. Çalık A, Dokuzlar O, Uçar N (2020) The effect of heat treatment on mechanical properties of 42crmo4 steel. J Achiev Mater Manuf Eng 98:5–10. https://doi.org/10.5604/01.3001.0014.0811
38. Ulrich C, Günther S, Becker N, et al (2025) High strength tempered 42CrMo4 for shafts in drive technology. Forsch im Ingenieurwes 2025 891 89:59-. https://doi.org/10.1007/s10010-025-00818-x
39. Xu Q, Zhao J, Ai X (2017) Cutting performance of tools made of different materials in the machining of 42CrMo4 high-strength steel: a comparative study. Int J Adv Manuf Technol 93(5 93):2061–2069. https://doi.org/10.1007/s00170-017-0666-6
40. Yildirim ÇV, Kivak T, Sarikaya M, Şirin Ş (2020) Evaluation of tool wear, surface roughness/topography and chip morphology when machining of Ni-based alloy 625 under MQL, cryogenic cooling and CryoMQL. J Mater Res Technol 9:2079–2092. https://doi.org/10.1016/j.jmrt.2019.12.069
41. Gross D, Appis M, Hanenkamp N (2019) Investigation on the productivity of milling ti6al4v with cryogenic minimum quantity lubrication. MM Sci J 2019:3393–3398. https://doi.org/10.17973/mmsj.2019_11_2019098
42. Sterle L, Mallipeddi D, Krajnik P, Pušavec F (2020) The influence of single-channel liquid CO2 and MQL delivery on surface integrity in machining of Inconel 718. In: Procedia CIRP. Elsevier B.V., pp 164–169. https://doi.org/10.1016/j.procir.2020.02.032
43. Grguraš D, Sterle L, Krajnik P, Pušavec F (2019) A novel cryogenic machining concept based on a lubricated liquid carbon dioxide. Int J Mach Tools Manuf 145:1–6. https://doi.org/10.1016/j.ijmachtools.2019.103456
44. Arunkarthikeyan K, Balamurugan K, Rao PMV (2020) Studies on cryogenically treated WC-Co insert at different soaking conditions. Mater Manuf Process 35:545–555. https://doi.org/10.1080/10426914.2020.1726945
45. Akincioğlu S, Gökkaya H, Uygur İ (2015) A review of cryogenic treatment on cutting tools. Int J Adv Manuf Technol 78:1609–1627. https://doi.org/10.1007/s00170-014-6755-x
46. Johansson D, Hägglund S, Bushlya V, Ståhl JE (2017) Assessment of Commonly used Tool Life Models in Metal Cutting. Procedia Manuf 11:602–609. https://doi.org/10.1016/j.promfg.2017.07.154
47. Oraby SE, Hayhurst DR (1991) Development of models for tool wear force relationships in metal cutting. Int J Mech Sci 33:125–138. https://doi.org/10.1016/0020-7403(91)90062-8
48. Vrabeľ M, Paľo M, Semanová M et al (2020) Tool condition monitoring when hard machining. Acta Mech Slovaca 24:20–28. https://doi.org/10.21496/AMS.2020.019
49. Grzesik W, Bartoszuk M, Nieslony P (2005) Finite element modelling of temperature distribution in the cutting zone in turning processes with differently coated tools. J Mater Process Technol 164:1204–1211. https://doi.org/10.1016/j.jmatprotec.2005.02.136
50. Anagonye AU, Stephenson DA (2002) Modeling Cutting Temperatures for Turning Inserts With Various Tool Geometries and Materials. J Manuf Sci Eng 124:544–552. https://doi.org/10.1115/1.1461838
51. Cichosz P, Karolczak P, Waszczuk K (2023) Review of cutting temperature measurement methods. Mater 2023:6365. https://doi.org/10.3390/ma16196365
52. Lauro CH, Brandão LC, Baldo D et al (2025) Temperature Measurement with Indexable Inserts via Functional Coating in Turning Processes. Procedia CIRP 134:247–252. https://doi.org/10.1016/j.measurement.2014.08.035
53. Javaraiah RM, Suresh SK, Narayana SH, et al (2024) Comparative Study on Temperature Measurement of a Coated and Uncoated Tool Insert in Turning Process by Using Tool Work Thermocouple. AIP Conf Proc 3060:. https://doi.org/10.1063/5.0197020
54. Aslantas K, Hasçelik A, Erçetin A et al (2024) Effect of cutting conditions on tool wear and wear mechanism in micro-milling of additively manufactured titanium alloy. Tribol Int 193:109340. https://doi.org/10.1016/j.triboint.2024.109340
55. Suárez A, Veiga F, Sandua X et al (2025) Machinability of Waspaloy: an investigation of cutting forces and tool wear in turning. Int J Adv Manuf Technol 2025:3159–3172. https://doi.org/10.1007/S00170-025-15983-0
56. Burnett ES (1923) Experimental study of the Joule-Thomson effect in carbon dioxide. Phys Rev 22:590. https://doi.org/10.1103/PhysRev.22.590
57. Röckelein A, Meier T, Hanenkamp N (2025) Optimization of the CO2 Supply of a Cryogenic Minimum Quantity Lubrication System for Machining Processes. Lect Notes Mech Eng 381–389. https://doi.org/10.1007/978-3-031-93891-7_42
58. Sadílek M, Dubský J, Sadílková Z, Poruba Z (2016) Cutting forces during turning with variable depth of cut. Perspect Sci 7:357–363. https://doi.org/10.1016/j.pisc.2015.11.055

59. Cakir MC, Ensarioglu C, Demirayak I (2009) Mathematical modeling of surface roughness for evaluating the effects of cutting parameters and coating material. J Mater Process Technol 209:102–109. https://doi.org/10.1016/j.jmatprotec.2008.01.050
60. Cappellini C, Abeni A (2022) Development and implementation of crater and flank tool wear model for hard turning simulations. Int J Adv Manuf Technol 120:2055–2073. https://doi.org/10.1007/s00170-022-08885-y
61. Sarikaya M, Gupta MK, Tomaz I et al (2021) A state-of-the-art review on tool wear and surface integrity characteristics in machining of superalloys. CIRP J Manuf Sci Technol 35:624–658. https://doi.org/10.1016/j.cirpj.2021.08.005
62. Barzegar Z, Ozlu E (2021) Analytical prediction of cutting tool temperature distribution in orthogonal cutting including third deformation zone. J Manuf Process 67:325–344. https://doi.org/10.1016/j.jmapro.2021.05.003
63. Li W, Zhou B, Xing L et al (2023) Influence of cutting parameters and tool nose radius on the wear behavior of coated carbide tool when turning austenitic stainless steel. Mater Today Commun 37:107349. https://doi.org/10.1016/j.mtcomm.2023.107349
64. Llanos I, Urresti Espilla I, Bilbatua D, Zelaieta O (2024) Evaluation of sustainability and cost effectiveness of using LCO2 as cutting fluid in industrial hard-turning installations. Sustain 2024:10078. https://doi.org/10.3390/SU162210078
65. Davies MA, Ueda T, M'Saoubi R et al (2007) On the measurement of temperature in material removal processes. CIRP Ann Manuf Technol 56:581–604. https://doi.org/10.1016/j.cirp.2007.10.009
66. Davies MA, Cao Q, Cooke AL, Ivester R (2003) On the measurement and prediction of temperature fields in machining AISI 1045 steel. CIRP Ann 52:77–80. https://doi.org/10.1016/S0007-8506(07)60535-6